ECS Transactions, 58 (7) 127-133 (2013)
10.1149/05807.0127ecst ©The Electrochemical Society

How to Dope a Semiconductor Nanocrystal

Yorai Amit,[a,b] Adam Faust, [a,b] Oded Millo,[b,c] Eran Rabani,[d] Anatoly I. Frenkel,[e] and Uri Banin*[a,b]

[a]The Institute of Chemistry, [b]The Center for Nanoscience and Nanotechnology, and [c]The Racah Institute of Physics, , Hebrew University, Jerusalem 91904, Israel
[d]School of Chemistry, Sackler Faculty of Exact Sciences, Tel Aviv University, Tel Aviv 69978, Israel
[e]The Department of Physics, Yeshiva University, New York, New York 10016, United States
*To Whom Correspondence should be addressed. E-mail: uri.banin@mail.huji.ac.il

The doping of colloidal semiconductor nanocrystals (NCs) presents an additional knob beyond size and shape for controlling the electronic properties. An important problem for impurity doping is associated with resolving the location and structural surrounding of the dopant within the small NCs, in light of tendency for driving of the impurity atom to the surface of the NC. A post-synthesis diffusion-based doping approach for introducing metal impurities into InAs NCs is described and characterized. This enables accurate correlation between the emerged electronic properties and the doping process. Optical absorption spectroscopy and scanning tunneling spectroscopy (STS) measurements revealed the n-type and p-type behavior of the doped NCs, depending on the identity of selected impurities. X-ray absorption fine structure (XAFS) spectroscopy measurements demonstrated the interstitial location of Cu within the InAs NCs, acting as an n-type dopant, which was found to occupy a single unique hexagonal interstitial site within the NC lattice for a wide range of doping levels.

Introduction

Doping of semiconductor materials enables manipulation of their electronic properties. This is achieved by introducing an impurity atom into the crystal lattice, which in turn changes the free carrier distribution and affects the conductivity of the material. The ability to control the electrical characteristics of bulk semiconductors is the basis for the fabrication of microelectronic and optoelectronic devices such as field effect transistors (FETs) and diodes, which are the corner stone for numerous technologies. Although semiconductor nanocrystals (NCs) are well known for their size dependent electronic properties [1], which already resulted in various demonstrations of NC based applications such as light-emitting diodes [2,3], solar-cells [4], and transistors [5], the prospect of doping in semiconductor NCs, as an additional knob for controlling their electronic properties, is still widely pursued [6]. The concept of impurity doping in NCs is far more complex than in bulk semiconductors and was considered to be governed by three main factors: the NC surface morphology, the NC shape, and the capping ligands [7]. However, these factors address the isovalent impurity doping wherein the doped NCs were

Downloaded on 2013-11-13 to IP 132.66.153.86 address. Redistribution subject to ECS license or copyright; see ecsdl.org/site/terms_use

synthesized following a high-temperature reaction by adding the impurity precursors to the synthesis vessel [8]. Additional factors should be considered when attempting to perform aliovalent doping, where issues such as the stability of the impurity within the NC, the impurity site within the lattice, and the interaction between the two species, strongly contribute to the induced electronic effects. Figure 1 illustrates two cases of aliovalent impurity doping in an InAs lattice (figure 1,a). The n-type doping scheme illustrates an interstitial impurity (figure 1,b) that donates an electron to the NC. For such a case, Cu may be used given its small size and diffusion characteristics in III-V bulk semiconductors [9]. The second scheme illustrates an Ag atom substituting for the central In cation (figure 1,c). The Ag impurity would then generate free holes in the NC lattice, due to the lack of valence electrons compared with the native In atom, making the NC p-type

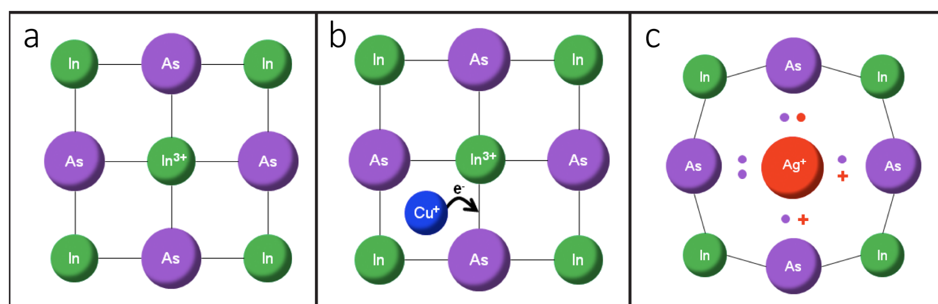

Figure 1. Illustration of impurity doping in InAs NCs. (a) A simplified model of the InAs lattice wherein the In atom has a +3 oxidation state. (b) An InAs lattice with an interstitial Cu impurity donating a valance electron to the lattice, thus yielding an n-type semiconductor. (c) An InAs lattice with a substitutional Ag impurity acting as an acceptor due to the lack of valance electrons, thus yielding a p-type semiconductor.

An additional method for electronic doping in semiconductor NCs was demonstrated through a process of electron-transfer, referred to as ‘remote-doping’. This was achieved by exposing the NCs to an electron donor on its surface (such as sodium-biphenyl), which donates an electron to the NC and therefore renders it n-type [10]. Even though this process seems to bypass the issues of stabilization regarding the impurity atom in the NC, it remains a challenge to achieve high control for both p-type and n-type doping. As noted above, semiconductor NCs are well-known for their size dependent electronic properties. Therefore, yet another problematic aspect of impurity doping when it comes to NCs is the ability to ascertain the electronic effect, caused solely by the introduction of the impurity atom. To this extent, different post-synthesis doping methods were proposed [11,12], demonstrating changes in the electronic properties of the NC-based devices upon doping. Nevertheless, the location and stability of the impurity within the NC lattice are still undetermined. Here we describe and summarize our approach for the aliovalent impurity doping of InAs NCs providing heavily doped semiconductor nanocrystals, and discuss the synthesis, optical and electronic properties, and structural characterization [13,14].

Doping of Colloidal InAs Nanocrystals in Solution

We utilized a facile, post-synthesis, room temperature, solution-phase reaction for introducing metal impurities into the lattice of the NC in a highly controlled manner. The doping of the colloidal InAs NCs was achieved by mixing the NC solution, comprised of

Downloaded on 2013-11-13 to IP 132.66.153.86 address. Redistribution subject to ECS license or copyright; see ecsdl.org/site/terms_use

colloidal InAs NCs dispersed in toluene, and impurity solution, which consists of metal salts, such as $CuCl_2$ and $AgNO_3$, and the appropriate accompanying agents and ligands, i.e. didodecyldimethylammonium bromide (DDAB) and dodecylamine (DDA) dissolved in toluene, at known volume fractions. Upon mixing the two solutions, the impurity diffusion to the surface of the NC is mediated by the chosen ligands, previously suggested in the ‘trapped-dopant model’ [15], and the impurities then diffuse into the NC lattice.

Several changes in the optical and electronic properties were observed upon doping, which reflects the situation of “heavy doping”. The different electronic effects are summarized in figure 2. The optical absorption spectra (figure 2,a) of the 3.3 nm InAs NCs shows a shift in the band-gap energy of the as-synthesized InAs NCs (black) when doped with either Cu (blue) or Ag (red). As illustrated in figure 1, the Cu and Ag induce different electronic properties when introduced into the InAs NC. The blue shift in the absorption spectra upon doping with Cu correlates to the band edge filling by donated impurity electrons, consistent with n-type doping. The red shift in the band-gap energy is associated with the Moss-Burstein and is consistent with the expected behavior of a p-type dopant.

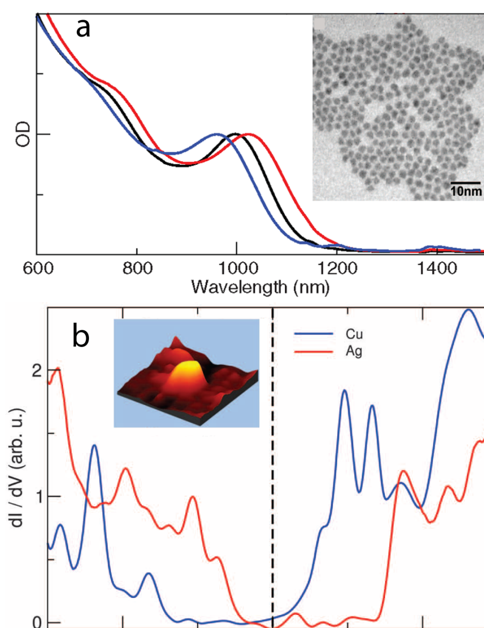

Figure 2. The effect doping on the electronic properties of InAs NCs. (a) Optical absorption spectra of Cu-doped (blue) and Ag-doped (red) InAs NCs shows a blue, red shift in the band-gap energy compared to that of the un-doped InAs NCs (black), respectively. Inset, TEM image of the Ag-doped 3.3 nm InAs NCs. (b) STM tunneling spectra at 4.2K of Cu-doped (blue) and Ag-doped (red) InAs NCs shows the relative shifts of the band gap edges with respect to the 0V bias (dashed line) indicating n-type and p-type character, for Cu and Ag, respectively. Inset, STM image of a single Ag-doped InAs NC.

The electronic characteristics the dopants have on the NCs can also be seen in the STS measurements (figure 2,c). The presented dI/dV-V curves correspond to the density of states in the scanned NC (figure 2,d). It is clearly seen that, whereas Cu doping (blue) shifts the conduction band maximum closer to the 0V bias - a prototypical effect of n-type doping, the Ag doping (red) shifts the valence band minimum closer to the 0V bias, a clear indication of p-type doping. Figure 2,b shows the TEM image of the Ag doped

Downloaded on 2013-11-13 to IP 132.66.153.86 address. Redistribution subject to ECS license or copyright; see ecsdl.org/site/terms_use

InAs NCs. From this we deduce the NCs maintained their structural aspects and eliminate the possibility of size effects governing the observed optical shifts.

Determining the Impurity Location; The Case of Cu in InAs

In order to address the issues of identifying the location of the impurity and its stability within the NCs, the electronic state and structural aspects of the impurity atom embedded within the NC were investigated [14]. We employed advanced characterization methods of extended x-ray absorption fine structure (EXAFS) and x-ray absorption near edge structure (XANES) spectroscopies, which are complementary methods for structural characterization of nanoscale materials, to reveal the impurity site and its concentration dependence for a series of Cu doped, 5 nm InAs NC samples. Figure 3 presents the XANES (figure 3, a-c) and EXAFS (figure 3, d-f) results of the as-synthesized InAs NCs and of these InAs NCs doped with various concentrations of Cu. The position of the absorption edge is depicted by the main peak of the XANES spectra, which corresponds to the 1s – 4p electronic transition for As and Cu K-edges (figure 3,a and c, respectively) and the 1s – 5p electronic transition for In K-edge (figure 3,b). The position of this peak is sensitive to the charge state of the absorber and therefore indicates that the charge state of both In and As atoms do not change upon doping with a wide range of Cu concentrations. The increase in the area under the peak, known as the white-line (WL), is indicative of an increase in the number of nearest neighbors with increasing the Cu concentration.

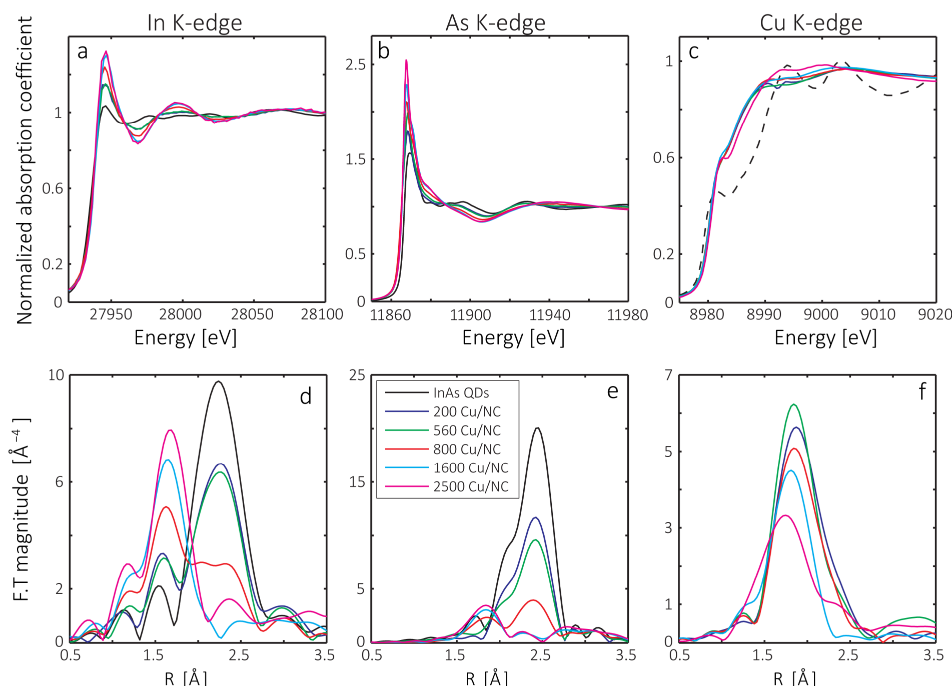

Figure 3. In, As, and Cu K-edge XANES spectra (a-c, respectively) and the Fourier transform (FT) magnitudes of their EXAFS spectra (d–f, respectively) measured for Cu-doped 5 nm InAs NCs, measured at the In K-edge (left frames (a,d)), As K-edge (center frames (b,e)), and Cu K-edge (right frames (c,f)). Dashed line (c) shows the XANES spectra for Cu(0) (black) standard. The legend in frame (e) refers to all the graphs, and all stated doping levels relate to the doping level in solution.

Downloaded on 2013-11-13 to IP 132.66.153.86 address. Redistribution subject to ECS license or copyright; see ecsdl.org/site/terms_use

The relatively constant position and shape of the Cu K-edge XANES spectra suggest that for all measured doping levels the Cu impurities occupy similar lattice sites and have similar charge states. Furthermore, the XANES spectrum of the Cu K-edge is notably different than that of the metallic Cu (figure 3, c, dashed-line), indicating the increase in the nature of covalent bonding, compared with pure Cu, between the impurity atom and the lattice. The EXAFS portion of the spectra reflects details concerning the location and surrounding structure of the absorbing atom. Examination of the In and As K-edge EXAFS spectra, as measured for different Cu doping concentrations reveals a change in the surrounding structure before, and after, doping with Cu. The un-doped InAs sample (black) exhibits initially a single peak in the EXAFS spectrum, indicative of a single nearest neighbor distance, consistent with the expected contribution from the In-As pair in a zincblende structure. However, upon doping, a second peaks is formed, and although the relative contributions of the In-As(As-In) and In-Cu(As-Cu) change with increasing Cu concentrations, the lateral position of both peaks is constant throughout. This suggests that (i) the Cu impurities occupy a lattice site with a mean In-Cu (As-Cu) bond length distance that is shorter than the zincblende In-As bond length and (ii) it does not affect the native In-As zincblende characteristics. These two conditions can coexist only if the Cu occupies an interstitial lattice site. From the Cu K-edge EXAFS spectra we deduce that the Cu is located in a unique lattice site characterized by an identical inter-atomic distances to both In and As nearest neighbors. Contemplating all of the above indicated towards a single possible site for the Cu impurity – a hexagonal interstitial lattice site. Figure 4 illustrates the 3D structural model of a zincblende unit-cell for Cu doped InAs NCs. The side-view (figure 4,a) and the top-view (figure 4,b) indicate the Cu atom is located in the center of the hexagonal ring. This site is characterized by three In and three As surrounding atoms with an identical bond length distance of 2.5 Å. This results in a similar contribution from either Cu-In or Cu-As pairs to the EXAFS signal, which leads to the formation of a single peak for all doping levels. This interstitial site for the Cu impurities then explains the n-type character in this case, as schematically illustrated in figure 1b, and leads to the electronic characteristics described above and illustrated in figure 2.

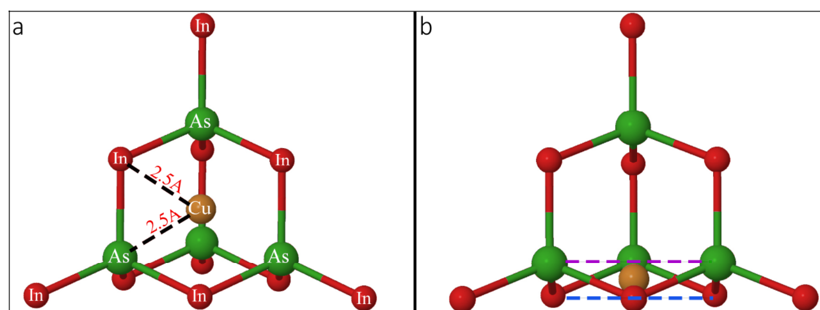

Figure 4. Illustrations of a Cu impurity (orange) in an InAs (red, green respectively) NC of a zincblende structure. Top view (a) and side-view (b) of the interstitial hexagonal site: The impurity is positioned at ([3/8, 3/8, 5/8]*a). Coordination numbers of both Cu-In and Cu-As have theoretical values of three, and a mean inter-atomic bond length of 2.5 Å.

.

Downloaded on 2013-11-13 to IP 132.66.153.86 address. Redistribution subject to ECS license or copyright; see ecsdl.org/site/terms_use

Conclusions

Impurity doping in colloidal semiconductor NCs opens the door for post-synthesis manipulation of the electronic properties to produce both n-type and p-type NCs. Following the diffusion-based doping approach gives exquisite control over the impurity concentration within the NC in a highly reproducible manner. The structural analysis revealed that for Cu doped InAs NCs, the impurity occupies a unique site within the NC lattice, regardless of the impurity concentration. Utilizing this approach will greatly facilitate in studying the dynamics of impurity doping in semiconductor NCs, as well as correlating between the resulting electronic properties and the unraveled structural aspects. The availability of n-type and p-type doped NCs, opens the path for further control of NC-based electronic and optoelectronic devices prepared via facile bottom-up fabrication methods.

Downloaded on 2013-11-13 to IP 132.66.153.86 address. Redistribution subject to ECS license or copyright; see ecsdl.org/site/terms_use

Acknowledgments

The research leading to these results has received funding from the European Research Council under the European Union's Seventh Framework Programme (FP7/2007-2013)/ERC grant agreement No. 246841. AIF acknowledge the support of this work by the U.S. DOE Grant No. DE-FG02-03ER15476. X18B beamline is supported, in part, by Synchrotron Catalysis Consortium (U. S. DOE Grant No. DE-FG02-05ER15688). UB thanks the Alfred and Erica Larisch Memorial Chair and OM thanks the Harry de Jur Chair in Applied Science.

References

1. A. A. Guzelian; U. Banin; A. V. Kadavanich; X. Peng; A. P. Alivisatos;. *App. Phys. Lett.*, **69**, (1996).
2. S. Coe; W.-K. Woo; M. Bawendi; V. Bulovic *Nature*, **420**, (2002).
3. M. Soreni-Harari; D. Mocatta; M. Zimin; Y. Gannot; U. Banin; N. Tessler;. *Adv. Func. Mater.*, **20**, (2010).
4. I. Gur; N. A. Fromer; M. L. Geier; A. P. Alivisatos;. *Science*, **310**, (2005).
5. D. V. Talapin; C. B. Murray *Science*, **310**, (2005).
6. D. J. Norris; A. L. Efros; S. C. Erwin *Science*, **319**, (2008).
7. S. C. Erwin; L. Zu; M. I. Haftel; A. L. Efros; T. A. Kennedy; D. J. Norris *Nature*, **436**,(2005).
8. D. J. Norris; N. Yao; F. T. Charnock; T. A. Kennedy *Nano Letters*, **1**, (2000).
9. R. Dalven *Infrared Phys.*, **9**, (1969).
10. M. Shim; P. Guyot-Sionnest *Nature*, **407**, (2000).
11. S. M. Geyer; P. M. Allen; L.-Y. Chang; C. R. Wong; T. P. Osedach; N. Zhao; V. Bulovic; M. G. Bawendi *ACS Nano*, **4**, (2010).
12. J.-H. Choi; A. T. Fafarman; S. J. Oh; D.-K. Ko; D. K. Kim; B. T. Diroll; S. Muramoto; J. G. Gillen; C. B. Murray; C. R. Kagan *Nano Letters*, **12**, (2012).
13. D. Mocatta; G. Cohen; J. Schattner; O. Millo; E. Rabani; U. Banin *Science*, **332**, (2011).
14. Y. Amit; H. Eshet; A. Faust; A. Patllola; E. Rabani; U. Banin; A. I. Frenkel *The J. Phys. Chem. C*, **117**, (2013).
15. M.-H. Du; S. C. Erwin; A. L. Efros *Nano Letters*, **8**, (2008).

Downloaded on 2013-11-13 to IP 132.66.153.86 address. Redistribution subject to ECS license or copyright; see ecsdl.org/site/terms_use